

Research Article

Response of Step-Like Landslide to Pore-Water Pressure under the Action of Typhoon and Rainstorm

Zhijie Huang ¹, Wenbin Jian ^{1,2}, Qingling Liu ¹ and Hongqiang Dou ^{1,2}

¹Department of Geotechnical and Geological Engineering, Fuzhou University, Fuzhou, Fujian 350108, China

²Engineering Research Center of Geological Engineering, Fuzhou University, Fuzhou, Fujian 350108, China

Correspondence should be addressed to Wenbin Jian; jwb@fzu.edu.cn

Received 25 July 2022; Accepted 25 October 2022; Published 3 November 2022

Academic Editor: Yu Wang

Copyright © 2022 Zhijie Huang et al. This is an open access article distributed under the Creative Commons Attribution License, which permits unrestricted use, distribution, and reproduction in any medium, provided the original work is properly cited.

Step-like landslides have been attracting more and more attentions because of their displacement with step-like characteristics. At present, there are few studies about the mechanism of a step-like landslide from the perspective of its response to pore-water pressure. This paper considers the Yaoshan landslide disaster mainly affected by rainfall and groundwater in Anxi County, Quanzhou City, Fujian Province, as an example. Based on an in situ monitoring test, we explored the infiltration pathways of typhoons and rainstorms, the main influencing factors, and characteristics of pore-water pressure and determined the relationship between landslide displacement and pore-water pressure in the study area. The results show the following: (1) the pore-water pressure within the slope varies with fluctuation in groundwater level which is influenced by vertical infiltration of rainwater through the slope surface and dominant channels in the study area. (2) The landslide exactly produces a step-like displacement when the pore-water pressure near the slip surface increases from the minimum point to the maximum and then dissipates to the vicinity of the starting point. (3) The correlation between pore-water pressure change and landslide displacement is revealed, and the empirical formula that can characterize slope displacement generated by increment in per unit of pore-water pressure in unit time has been proposed. This study is crucial as it offers important theoretical and practical significance for the analysis of disaster-causing mechanism and monitoring and early warning of the same type of landslide.

1. Introduction

Landslide is a common geological disaster that not only causes serious damage to life and property but also brings serious damage to natural ecology and the environment. In the southeast coastal area of China, the slopes easily destabilize and slide under the influence of prolonged rainfall in spring and summer as well as typhoons causing a kind of downslope step-like displacement which is relatively typical [1–3]. At present, successful studies have been carried out on the mechanism of rainfall-induced landslides [4–8]. For example, the mechanism of the Shangwan landslide in Xining, Qinghai, was identified as the rapid increase in the slope moisture content due to rainfall and a decrease in shear strength due to water-rock interactions, according to the indoor experiments and numerical simulation [5]. The main inherent factor analyzed through model tests for the occurrence of traction landslide was the saturation of the soil

at the foot of the slope under the influence of rainfall [6]. However, studies on the mechanism of the step-like landslides have mainly focused on the reservoir-induced landslides while ignoring those landslides mainly caused by rainfall. For example, based on the monitoring data, the main reason for the occurrence of the Baijiabao step-like landslide in the Three Gorges reservoir area is thought to be the seepage pressure caused by the effective slope generated due to the difference between the groundwater level and the reservoir water level which drops periodically [9]. In summarizing 189 geological hazards in the Three Gorges reservoir area, the superimposed effects of a rapid decline of reservoir water level and rainstorms are considered as the main triggering factors for the landslides [10]. The initial reservoir storage, the combined effects of rainfall, and water level fluctuations in the reservoir are considered to be the main causes of the Zengjiapeng landslide in Fengjie and its successive multiple deformations [11]. The influence of

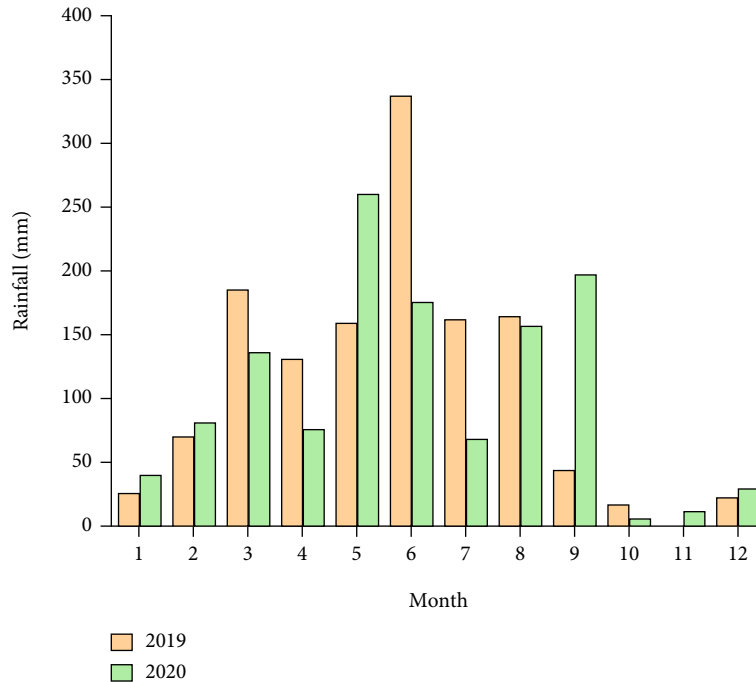


FIGURE 1: Monthly rainfall data of Xiping Town, Anxi County, 2019–2020.

pore-water pressure in causing a landslide has been emphasized by many researchers [12–15]. In a step-like landslide that is mainly affected by rainfall and groundwater, the pore-water pressure of slope material increases due to the rapid recharge by rainfall, having a direct influence on the magnitude and distribution of seepage forces along with the soil strength within the landslide body, which needs to be focused on [16–18].

For a better investigation of the mechanism of a step-like landslide under the action of rainfall and its effects on the groundwater and pore-water pressure, this paper focuses on the Yaoshan step-like landslide in Anxi County, Quanzhou City, Fujian Province. Based on an in situ monitoring test, the data of rainfall, moisture content, groundwater level, pore-water pressure, and landslide displacement were used to study the infiltration pathways of rainwater recharging pore-water pressure along with the influencing factors and characteristics of pore-water pressure and the response characteristics of displacement on pore-water pressure. The conclusions obtained from this study are of great significance in monitoring and developing an early warning system for step-like landslides.

2. Overview of Landslide in the Study Area

Anxi County, where the Yaoshan landslide is located, resides in the transition zone between the central subtropical and southern subtropical ocean monsoon climate, with a mild climate and abundant rainfall. The average annual rainfall is about ≈ 1500 mm–2000 mm, and in a few years, the rainfall has even reached up to 2900 mm. The rainfall data for Anxi County in the period ranging from January 2019 to Decem-

ber 2020 is shown in Figure 1. The rainfall is mainly concentrated from March to September, accounting for 81% of the average annual rainfall. In addition, Anxi County, which lies in the southeast coastal area of China, is also vulnerable to the impact of typhoon landing, such as typhoon “Bailu” in 2019 and typhoon “Mikra” in 2020, leading to heavy rainfall episodes and thereby increasing the probability of geological disasters in the study area.

The landslide disaster site is located in Yaoshan Village near Xiping Town of Anxi County, Fujian Province, China, which is shown in the location map of the study area (Figure 2). The study area is composed of tectonically eroded medium and low mountain landforms with the highest elevation of 957 m and the lowest elevation of 290 m. The Yaoshan landslide is located at the ridge in the middle and front of the slope with a longitudinal length of about 350 m, a trailing edge with a width of almost 80 m, and a front edge with a width of 200 m. Its surface area is approximately 5.2×10^4 m², and its shape on the plane looks like a “long tongue.” The slope of the landslide is about 20° to 25°. The Yaoshan landslide is a medium-sized soil landslide with a volume of about 50×10^4 m³. The slip surface has an approximate depth of 10 m to 13 m and is located near the interface between the top layer of colluvial gravel soil and the residual clay layer. According to the geological investigations, tension cracks are well developed at the trailing edge of the landslide, and the groundwater level is located above the slip surface all year round.

According to the data from the geotechnical engineering survey, the rock and soil masses in the landslide body from the top to the bottom are divided into the following main geotechnical layers: colluvial gravel soil, residual clay,

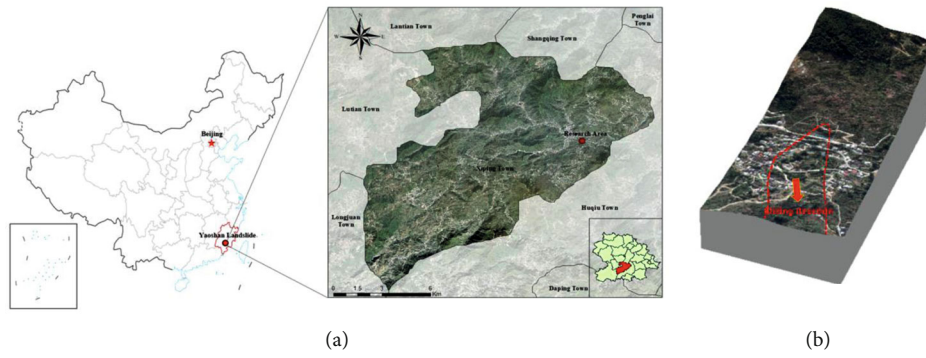


FIGURE 2: Location map and three-dimensional topographic map of the study area. (a) Location map. (b) Three-dimensional topographic map.

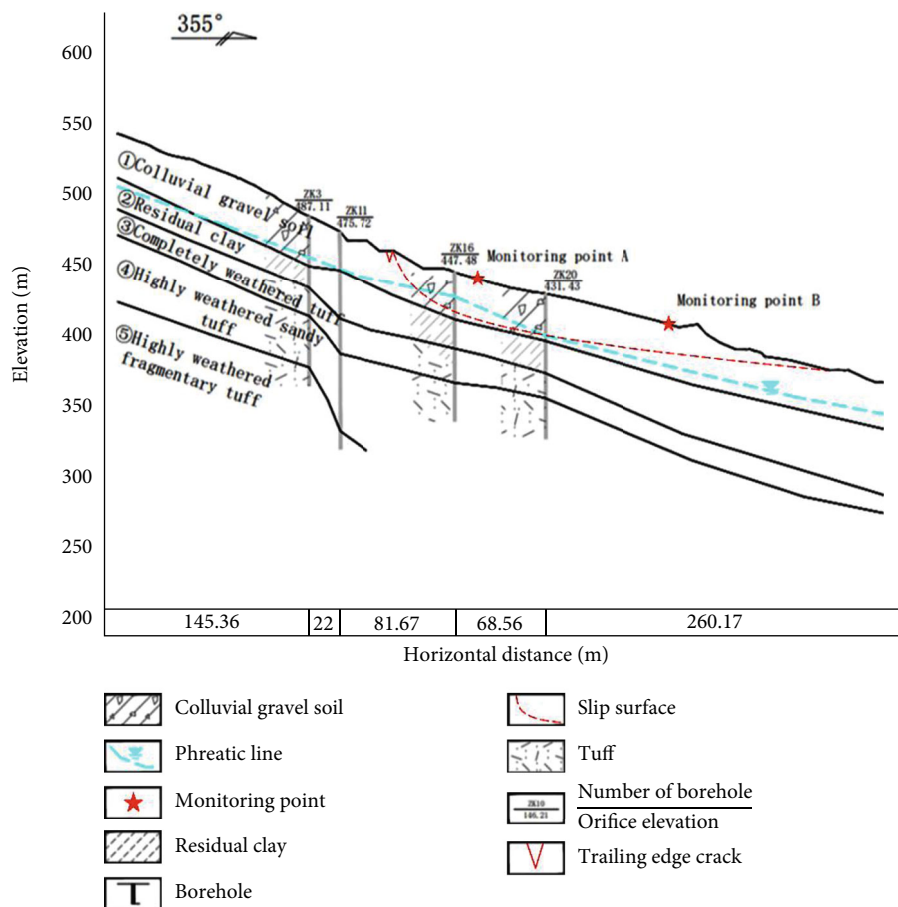


FIGURE 3: Geological section of the main landslide slip surface.

completely weathered tuff, highly weathered sandy tuff, and highly weathered fragmentary tuff. The geological profile of the main slip surface is shown in Figure 3.

3. In Situ Monitoring of Landslide

3.1. Monitoring Program. To achieve the research goal, a remote automatic monitoring test system was installed at the Yaoshan landslide zone in Anxi County, Fujian Province. Firstly, by selecting the location for installing the monitoring instrument and, secondly, by analyzing the recorded

data, the infiltration pathways of rainwater were revealed along with the other main influencing factors, characteristics of pore-water pressure, and the response features of the landslide. The results from the previous field survey and the photos of the landslide showed that the landslide depicted a tongue-shaped formation, with larger displacement in the middle part and smaller displacement on both sides of the landslide body. Therefore, point A in the middle part and point B in the lower part of the landslide was selected as instrumental monitoring point so that the recorded displacement data was much representative. The

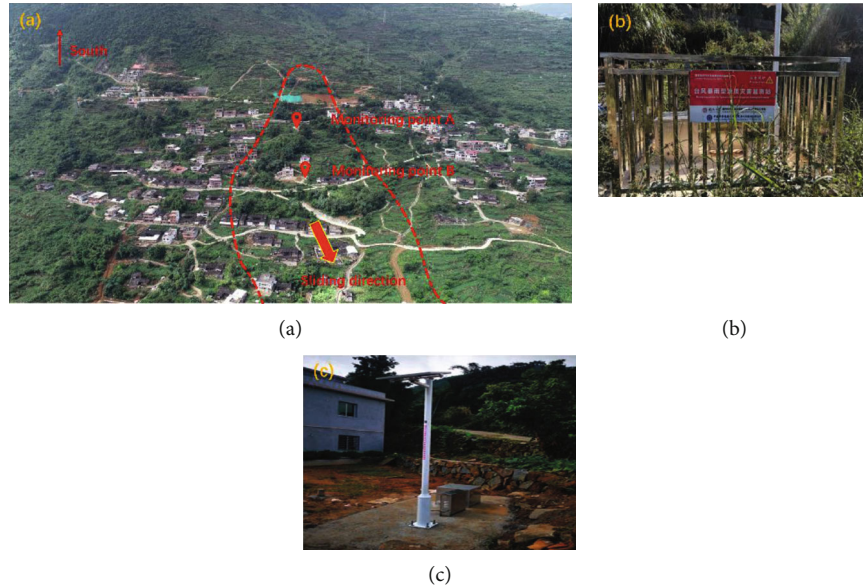


FIGURE 4: Schematic diagram of the landslide area and monitoring points. (a) Landslide area and monitoring point locations. (b) Monitoring point A. (c) Monitoring point B.

landslide deformation range and monitoring points A and B are shown in Figure 4, where the red dashed line represents the landslide deformation range, and the downward red arrow represents the sliding direction.

The main monitoring instruments used in the field testing are described in Table 1. For monitoring point A, a rain gauge was installed to record the real-time rainfall in the study area; a test pit was also excavated to install the probe moisture meters at a depth of 0.5 m, 1.0 m, 1.5 m, 2.0 m, 2.5 m, and 2.8 m to measure the moisture contents of the topsoil under the varying intensity of rainfall infiltration. Three boreholes were drilled to install the pore-water pressure gauges at 4.0 m, 5.8 m, and 10.0 m, respectively, to measure the pore-water pressure at various depths. A borehole was also drilled for fixed inclinometer installation at 4.0 m, 8.0 m, 10.0 m, 12.0 m, and 16.0 m depth, respectively, to measure the displacements. A water level meter was installed at the bottom of the last inclinometer to measure the groundwater level at monitoring point A. For monitoring point B, a test pit was excavated, and the probe moisture meters were installed at 0.5 m, 0.9 m, 1.3 m, 1.7 m, 2.1 m, and 2.5 m, respectively. Three boreholes were drilled, and the pore-water pressure gauges were installed at 4.0 m, 7.0 m, and 10.0 m, respectively. Another borehole was drilled at point B to install the fixed inclinometers at 4.0 m, 8.0 m, 10.0 m, 12.0 m, and 16.0 m depth, respectively, with a water level meter installed at the bottom of the last inclinometer measuring the groundwater level at point B. The instrument layout sections are shown in Figure 5.

3.2. Displacement Characteristics of Landslide in the Study Area. According to the field testing and monitoring data, the Yaoshan landslide is mainly affected by rainfall with step-like displacement characteristics. Figure 6 shows the relationship between the displacement near the slip surface at point A and rainfall data spanning from August 25,

2019, to September 25, 2020. It can be seen that the Yaoshan landslide, a typical step-like landslide greatly affected by rainfall, produces step-like displacement during the rainy period and produces constant displacement even with a little rain amount.

According to the meteorological data, the influence of heavy rainfall brought by typhoon “Bailu” in the study area on August 25, 2019, the landslide triggered a large displacement in a time period ranging from August 25, 2019, to August 30, 2019, in a step-like pattern. It began to rain in the early morning at 3:00 a.m. on August 25, 2019; therefore, the period from 3:00 a.m., August 25, to 300 a.m., August 30, was used to analyze the changes in soil moisture content, pore-water pressure, groundwater level, landslide displacement, and other related factors in the study area. This study reveals the infiltration pathways of rainwater and the influencing factors and characteristics of pore-water pressure, as well as other laws, of the step-like landslide in the study area under the influence of typhoons and rainstorms.

4. Results

4.1. Topsoil Moistures. Figure 7 shows the change in soil moisture content at monitoring point A of the landslide under the influence of rainfall activated by typhoon “Bailu.” Generally, the evaporation of water takes place from the topsoil; the deeper the soil layer is, the weaker the evaporation and the higher the soil’s initial moisture content. However, the landslide in the study area presented different features: at the stage before the start of rainfall, the reading of moisture meter 3 at a depth of 1.5 m was the highest, and the readings of moisture meters 4, 5, and 6 (respectively, with the depth of 2.0, 2.5, and 2.8 m) were relatively low. The lowest moisture reading was reflected by the moisture meter 4 (depth 2.0 m).

TABLE 1: List of main instruments.

	Rain gauge	Water level meter	Pore-water pressure gauge	Inclinometer	Moisture meter
Number of instruments	1	2	6	10	12
Manufacturer	Hunan Xiangyinhe Sensor Technology Co., Ltd.				
Measurement unit	mm	dm	kPa	Degree	%
Accuracy	0.1 mm	$\pm 0.1\%F.S$	$\pm 0.1\%F.S$	$\pm 0.05\%F.S$	$\pm 2\%F.S$
Resolution	0.01 mm	0.1 dm	0.1 kPa	0.01°	0.1%
Model	YH07-A01	YH04-A	YH04-B	YH01-B30	YH08-A
Symbol	RF	WL	PW	DI	MC
Measured physical quantity	Rainfall	Groundwater depth	Pore-water pressure	Deep displacement	Moisture content

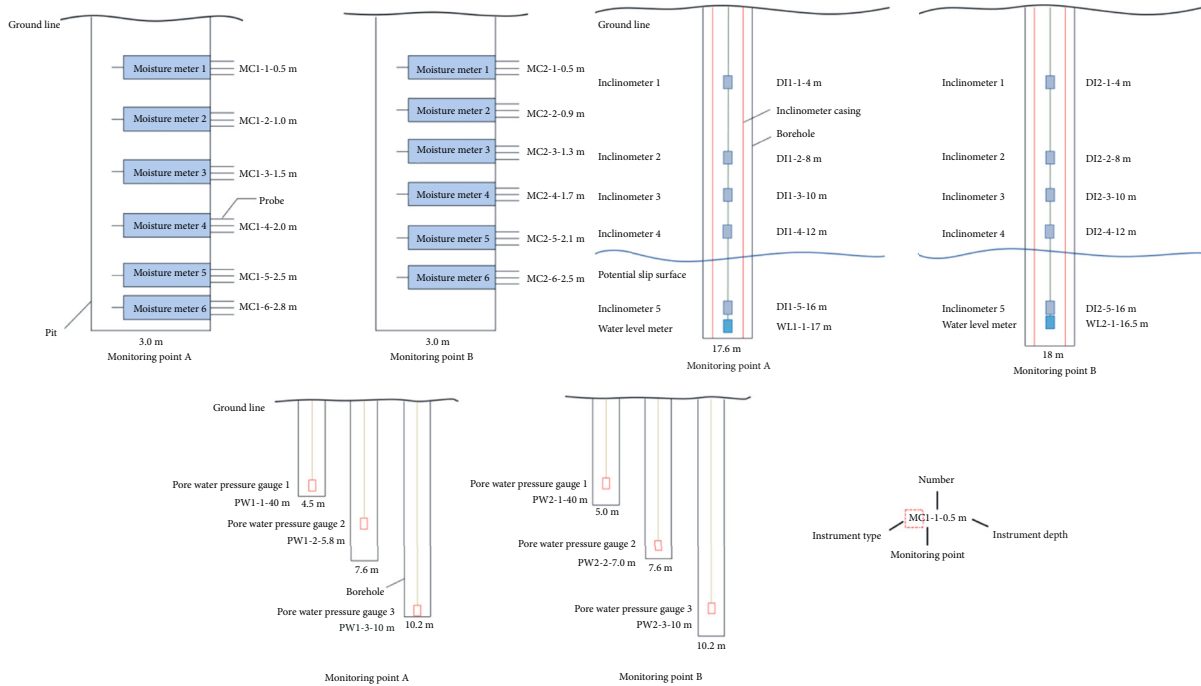


FIGURE 5: Sections of instrument layout at monitoring points.

As for the trend of moisture content with respect to the rainfall, the readings of moisture meters at different depths in the topsoil increased with the start of rainfall. It is worth noting that the reading of moisture meter 1 decreased at 2 h after the start of rainfall and then increased again at 3 h, followed by repeated fluctuations. Similarly, the reading of moisture meter 2 decreased at 4 h after the start of rainfall and then increased again at 10 h. However, the landslide body was recharged by rainfall during the above observation period. From the readings of moisture meters at different depths, it is worth noting that the readings of moisture meters 2 and 4 showed a rapid moisture increase at 2 h and 4 h after the start of rainfall, respectively. Comparatively, moisture meter 4 recorded a higher degree increase than that at moisture meter 2. From the perspective of response time, moisture meter 1 responded quickly after the rainfall started, and moisture meter 2 responded 2 h after the rainfall started showing a delay of 2 h. The response delay of moisture meter 3 was 3 h; however, the readings of moisture meters 4, 5, and 6 changed significantly at 4 h after the rainfall started, which

may be considered as their response delay period. It can be found that the response interval between moisture meters 1 and 2 and moisture meters 2 and 3 is at least 2 h, while the moisture meters 4, 5, and 6 responded at the same time. Therefore, the moisture meters 4, 5, and 6 reflected a response interval of 1 h with respect to moisture meter 3.

4.2. Groundwater Level. The groundwater levels at monitoring points A and B of the Yaoshan landslide at shallow depths are shown in Figure 8. In terms of the magnitude of the change in groundwater level at point A, the groundwater level was about 6.82 m before the rainfall. As the rainfall started, the level began to rise and reached its peak around 3.99 m, showing a change of approximately 3 m. For point B, the depth of groundwater level was about 1.88 m before rainfall. As the rainfall continued, the groundwater level began to rise and reached its peak of about 0.94 m with a variation of approximately 1 m. The response time of groundwater level to the rainfall was influenced by the depth of groundwater level and the longer seepage path at point A;

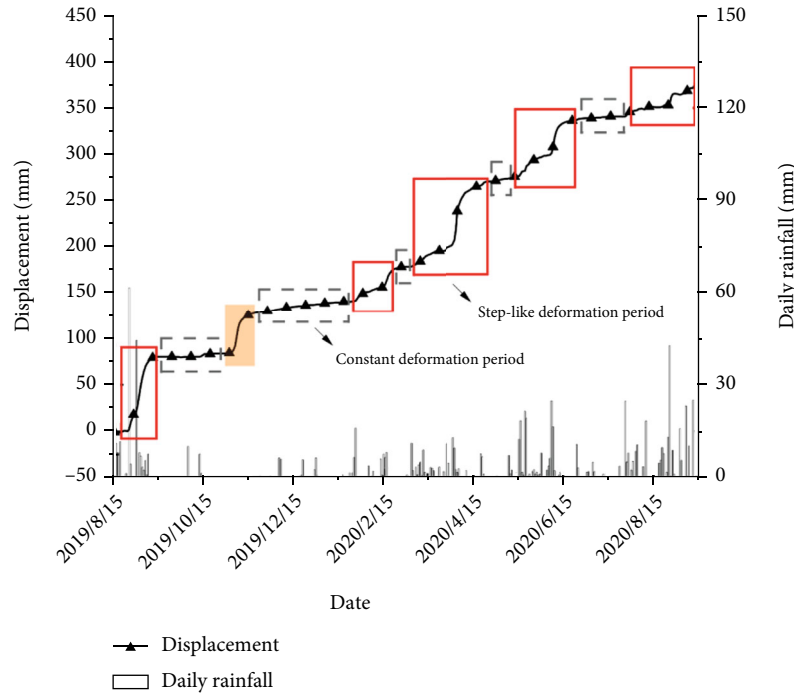


FIGURE 6: Relationship curve between rainfall and deep horizontal displacement at 12 m depth below the surface at point A in the study area.

therefore, the response time of groundwater level to rainfall at point A was 3 h and greater than that at the point B (i.e., 1 h).

The reason for the varying depths of the groundwater level at the two monitoring points is that point B is located at the lower part of the landslide. The main water-rich colluvial gravel soil layer and residual clay layer in this part are concave in shape, where the groundwater is easily obstructed and gathered, thus resulting in a higher groundwater level than that at point A. The higher groundwater level at point B makes the soil layer saturation much easier under rainfall, and the rainwater mostly gets discharged by the surface runoff, thus limiting the rise of the groundwater level at this location. For example, after the rainfall started, the slope of the groundwater level curve for the monitoring point A always remained at a large value. The groundwater level reached its peak because the amount of rainfall and its infiltration was not enough to keep the water table rising. However, the slope of the groundwater level curve at point B got smaller and smaller. The groundwater level reached its peak because the soil layer was already saturated, and the rainfall could no longer raise the groundwater level. Generally speaking, groundwater level changes will affect the pore-water pressure. The analysis on the groundwater level is to form a comparison with the pore-water pressure for better analyzing the influencing factors and characteristics of the latter.

4.3. Pore-Water Pressure. The pore-water pressure at monitoring points A and B of the Yaoshan landslide recorded during the study period is shown in Figure 9. Firstly, the change of pore-water pressure is closely related to the rainfall factor, and the pore-water pressure increased at both

the monitoring points and dissipated when there was little rainfall. For point A, the pore-water pressure at a depth of 4.0 m followed the same trend as the pore-water pressure at a depth of 5.8 m but varied at a depth of 10.0 m. The reason for this could be that before the rainfall in the study period, the soil layers at the former two depths were probably located above the groundwater level, while the soil layer at the latter depth was located below the groundwater level, which also influenced the pore-water pressure trend. Similarly, the groundwater level at point B was shallow, and the three pore-water pressure gauges PW2-1, PW2-2, and PW2-3 were all below it; therefore, the response time to rainfall was all less than 1 h, corresponding to the groundwater level response time. Besides, in general, the dissipation amplitude of pore-water pressure at point A was larger than that at point B, which also corresponded to the change in groundwater level at the two monitoring points.

4.4. Response Characteristics of Landslide Displacement to Pore-Water Pressure. Since the landslide's slip surface in the study area was below the groundwater level at a certain depth, the pore-water pressure was recorded at a depth of 5.8 m and 10 m near the slip surface at point A (both are located below the groundwater level), and the readings were used as the research objects to investigate the intrinsic factors of slope displacement near the slip surface. Two typical datasets containing step-like periods and constant periods, from April 1, 2020, 0:00 to May 10, 2020, 0:00 and June 7, 2020, 0:00 to July 10, 2020, 0:00, were selected for analysis, as shown in Figure 10. In general, the fluctuations in pore-water pressure due to the rise and fall of groundwater level are considered as direct factors causing the slope instability and producing step-like displacements in the study area,

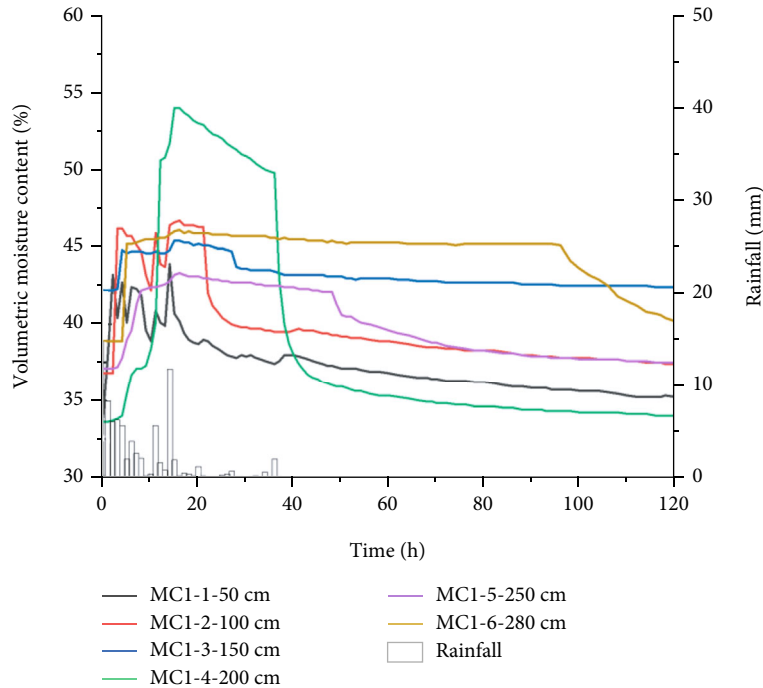


FIGURE 7: Relationship curve between rainfall and moisture contents at different depths of point A.

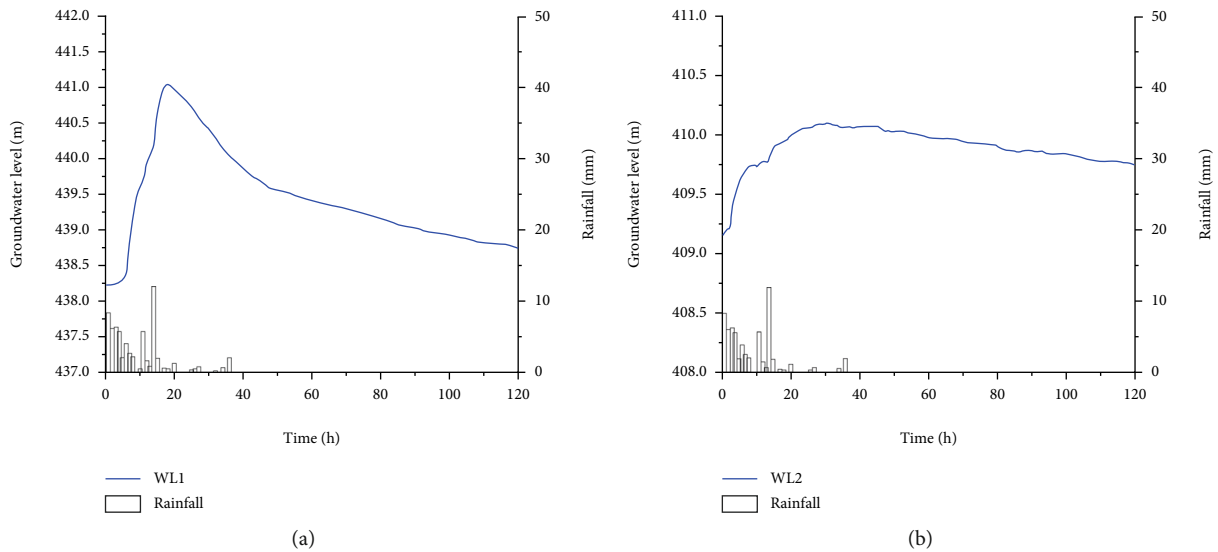


FIGURE 8: Relationship between rainfall and groundwater level during the study period. (a) Monitoring point A. (b) Monitoring point B.

showing a correlation between the change of pore-water pressure and the landslide displacement.

As shown in Figure 10(a), the Yaoshan landslide started to produce step-like displacement from 6:00 on April 2, as the pore-water pressure at a depth of 5.8m rose at 4:00 on April 2 and that at a depth of 10 m rose at 5:00 on April 2. So, the response time of the displacement near the slip surface to the pore-water pressure at a depth of 10 m was 1 h, which was smaller than its response time (i.e., 2 h) to the pore-water pressure at a depth of 5.8 m. Figure 10(b) also shows a similar pattern, and it can be inferred that, for the

pore-water pressure at different depths below the same groundwater level, the closer the distance between the displacement near the slip surface and the pore-water pressure at its upper boundary, the shorter the response time of the displacement to the pore-water pressure. Therefore, in the early warning analysis, it will be more theoretical and practical to select the factor of pore-water pressure near the slip surface and study the response of the slip surface displacement. The reason for this could be that the pore-water pressure near the slip surface is very similar to that at the slip surface. According to the effective stress principle, the degree

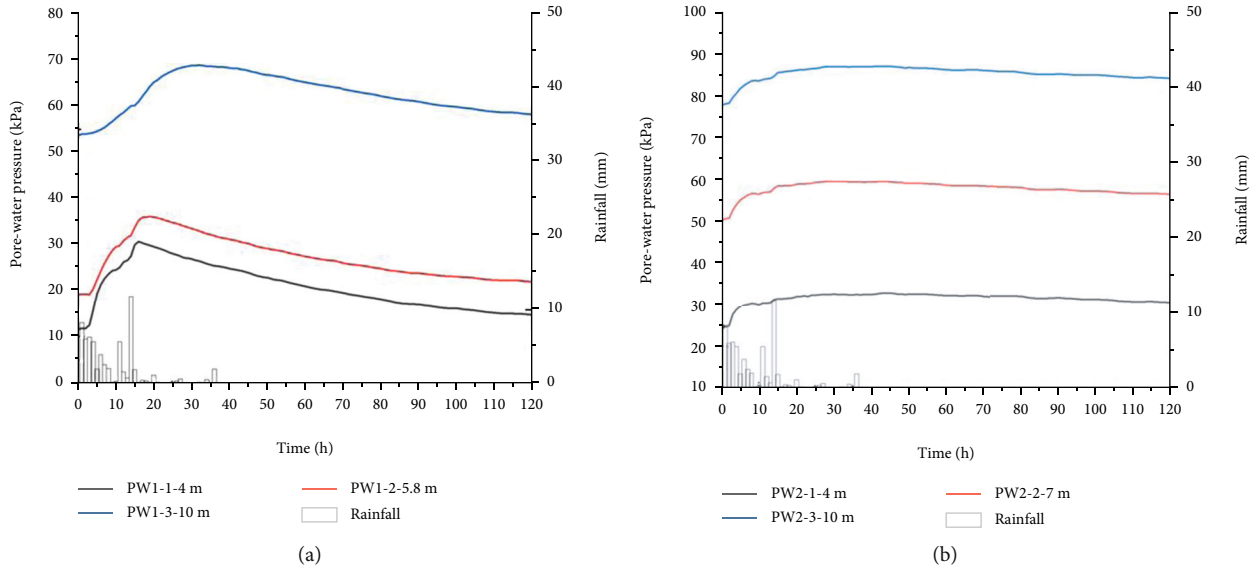


FIGURE 9: Relationship between rainfall and pore-water pressure during the study period. (a) Monitoring point A. (b) Monitoring point B.

of pore-water pressure will affect the shear strength of the soil, thus having an impact on the displacement and its response time. The closer the pore-water pressure to the real-time monitoring value, the more accurate the results are.

Another obvious characteristic in the figure is the relationship between the pore-water pressure at a depth of 10 m and the displacement near the slip surface, which was more regular than the pore-water pressure at a depth of 5.8 m. As shown in Figure 10(a), the pore-water pressure at a depth of 10 m increased from an initial value of 51.4 kPa to a peak value of 59.6 kPa and then dissipated to the vicinity of the starting value (51.6 kPa), corresponding to the whole step-like deformation period. As the pore-water pressure increased from the initial value to the peak one, the overall rate of displacement also increased (reflected in the increasing slope of the displacement curve); as the pore-water pressure dissipated from the peak, the overall rate of displacement started decreasing, and the landslide became stabilized. However, there is no relationship between the pore-water pressure at a depth of 5.8 m and the displacement. Figure 10(b) also shows a similar pattern. It also shows that it is more meaningful in landslide warning to select the pore-water pressure values in the vicinity of the slip surface for analysis.

5. Discussions

5.1. Rainwater Infiltration Pathways of Landslide in the Study Area. According to the monitoring results of topsoil moisture content along with geological investigations, it can be found that there are special characteristics in the readings and response time of moisture meters at different depths in the topsoil. The reason for this could be that there are many dominant channels formed by debris and vegetation roots in the topsoil of the study area have decayed (Figure 11), resulting in preferential rainwater flow through

the dominant channels to recharge the landslide subsurface after the surface infiltration. For example, (1) the initial readings of moisture meters 4, 5, and 6 were small, while the initial reading of moisture meter 3 was relatively the largest. This may be due to the presence of a dominant channel near the moisture meter 3, which has the preferential water flow causing a downward infiltration after the soil at the bottom of the channel is saturated. In other words, only when the soil at the bottom of the dominant channel (near the depth of moisture meter 3) is saturated due to rainfall, the rest of the water will infiltrate down to the depth of moisture meters 4, 5, and 6. (2) The phenomenon that the readings of moisture meters 1 and 2 first dropped and then increased again in the early stage of rainfall is not only related to the evaporation of topsoil but also is closely related to the process of water flow away from the specified depth due to the dominant channels in the soil layer. (3) The reading of moisture meter 4 increased rapidly in a short time of 4 h after the rainfall started. The reason behind this could be the large amount of moisture infiltration caused by the saturation of soil at a depth of the moisture meter 3 from which the probe of moisture meter 4 was exposed, resulting in a rapid rise in its reading. (4) Moisture meters 4, 5, and 6 responded simultaneously but were different from the response interval between rest of the moisture meters, which may result from a large amount of moisture infiltration after the saturation of a dominant channel.

In addition, at monitoring point A, the response time of pore-water pressure to rainfall at a depth of 4 m was 2 h while the response time of moisture content to rainfall at a depth of 2.8 m was 4 h. The reason for this could also be the existence of the trailing edge cracks and dominant channels in the Yaoshan landslide zone. Rainwater infiltrated through the cracks and dominant channels and reached the soil layer near the depth of 4 m, leading to pore-water pressure to respond at this depth before the vertical infiltration from the rainwater arrived. This phenomenon once

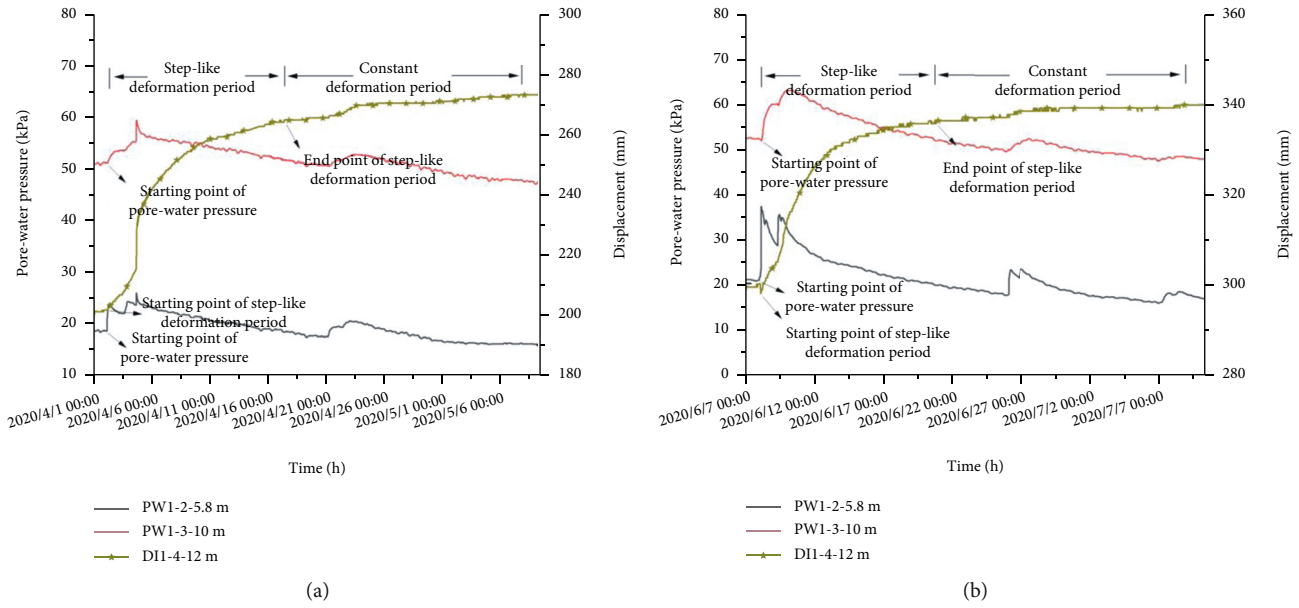


FIGURE 10: Relationship curve between displacement near the slip surface and pore-water pressure at different depths of point A in the study area. (a) April 1, 2020, 0:00~May 10, 2020, 0:00. (b) June 7, 2020, 0:00~July 10, 2020, 0:00.

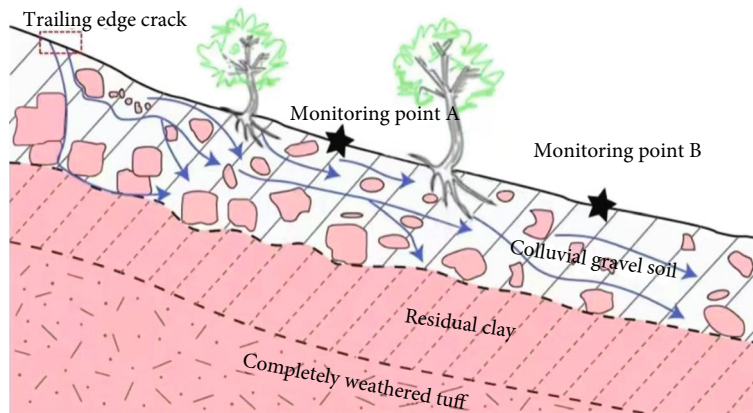


FIGURE 11: Groundwater dominant channels in the study area (adapted from [19]).

again supported the recognition that the dominant channels play an important role in rainfall infiltration, which has also been supported in a few previous studies [19–22].

5.2. Influencing Factors and Characteristics of Pore-Water Pressure. In light of the monitoring results of groundwater level and pore-water pressure, it can be found that, for the landslide in the study area, the groundwater level closely influences the change of pore-water pressure, which is mainly reflected in the following aspects: the trend of pore-water pressure below the groundwater level is very different from that above the groundwater level; the response time of pore-water pressure below the groundwater level to rainfall is consistent with the response time of the groundwater level; the dissipation amplitude of pore-water pressure at two monitoring points corresponds to that of the groundwater levels. Therefore, it can be inferred that there is a close rela-

tionship between the pore-water pressure and the groundwater level of the Yaoshan landslide. The change in pore-water pressure below the groundwater level is influenced by it to a greater extent.

5.3. Relationship between Displacement of Step-Like Landslide and Pore-Water Pressure. From the response characteristics of the step-like landslide displacement to pore-water pressure, there is a close relationship between landslide displacement and pore-water pressure. For example, it can be seen in Figure 10(a) that the pore-water pressure at a depth of 10 m had a small increase (about 4.2 kPa) near its peak, with a large growth (about 6.62 mm/h) in the landslide displacement rate during the monitoring period. For further analyzing the relationship between the pore-water pressure near the slip surface and the displacement rate, the pore-water pressure increments and displacement rates

TABLE 2: Analysis of pore-water pressure and displacement.

Time period	Pore-water pressure increment (kPa)	Displacement rate (mm/h)	Relative time interval	Influence degree (mm/h* kPa)
4.2 6:00–4.3 6:00	2.2	0.204	-0.803	0.093
4.3 6:00–4.4 6:00	1.4	0.232	-0.410	0.166
4.4 6:00–4.4 17:00	0.6	0.317	-0.123	0.528
4.4 17:00–4.4 19:00	4	6.620	-0.016	1.655
4.4 19:00–4.5 6:00	-2.7	0.697	0.018	0.258
4.5 6:00–4.9 6:00	-1.6	0.189	0.191	0.118
4.9 6:00–4.13 6:00	-1.5	0.058	0.502	0.039
4.13 6:00–4.17 16:00	-2.2	0.046	0.828	0.021

in different periods of pore-water pressure rise and dissipating stage (as shown in Table 2) were selected from Figure 10(a) for the analysis.

The pore-water pressure can affect the effective stress state of the soil, which in turn can affect the shear strength of the soil. Normally, the shear strength of the soil at the slip surface zone is in a residual state which makes the pore-water pressure change have greater influence on the movement and stability of it. In addition, the larger the value of pore-water pressure, the greater the influence of pore-water pressure on the stability and movement of soil. Therefore, in order to explore the influence of pore-water pressure on landslide movement at different time points during a rise and dissipating process of pore-water pressure, two concepts are defined below. Firstly, to strongly represent the interval between any time points corresponding to the peak pore-water pressure, the “relative time interval” is defined as the time from the midpoint of a period to the time corresponding to the peak pore-water pressure vs. the time the pore-water pressure rise or dissipation needs. As shown for PW1–3–10m of Figure 10(a), the negative sign indicated that the pore-water pressure was at a rising stage on the left side of the peak, and the positive sign indicated that the pore-water pressure was in the dissipating stage on the right side of the peak at this moment. Secondly, for analyzing the relationship between pore-water pressure increment and the displacement rate, the “influence degree” is defined as the displacement caused by pore-water pressure change in a certain period close to the peak value of pore-water pressure, which equals to the absolute displacement rate vs. pore-water pressure increment in a certain period. The “influence degree” can characterize the magnitude of displacement caused by each pore-water pressure increment per hour.

It can be found from the scatter plot presented in Figure 12 (prepared from the data in Table 2) that (1) in the rising stage of pore-water pressure, the displacement caused by per unit increase of pore-water pressure in unit time was significantly different from that in the dissipating stage. At the same relative time interval, each pore-water pressure increment in the rising stage caused a larger displacement in unit time than that in the dissipating stage. (2) Whether the pore-water pressure is in the rising stage or in the dissipating stage, the closer the pore-water pressure

to its peak, the larger displacement was caused by per unit of pore-water pressure increment in unit time and in the same time interval. (3) When the pore-water pressure began to dissipate from its peak, the displacement caused by per unit of pore-water pressure increment in unit time dropped rapidly in a very short period. According to the above analysis, the more dangerous situation is that the pore-water pressure increment drives the landslide to produce large displacement in a very short period which mainly occurred in the pore-water pressure rising stage near the peak. Whether there is a large displacement or not depends on the rise in pore-water pressure during that period. Therefore, when using the pore-water pressure for early warning of a landslide, the focus should be on the change in pore-water pressure near its peak.

For quantitatively analyzing the relationship between the influence degree of the pore-water pressure rise on the displacement and the relative time interval to the moment of peak pore-water pressure, the Asym2Sig function was used to fit the data points in Table 2. The inferred result is shown in Figure 12, which yields the following equation for the influence degree and relative time interval (the goodness of fit is 0.97839):

$$W = 0.08551 + 3.97747 \times \frac{1}{1 + e^{-(T-0.01201+0.64217 \times e^{-27})/0.0653}}} \times \frac{1-1}{1 + e^{-(T-0.01201-0.64217 \times e^{-27})/0.00249}}, \quad (1)$$

where T represents the relative time interval, i.e., the time from the midpoint of a period to the time point corresponding to the peak pore-water pressure vs. the time the pore-water pressure needs for a rise or dissipation (dimensionless), and W represents the influence degree of pore-water pressure increment on displacement (mm/h*kPa), which is the magnitude of displacement caused by each pore-water pressure rise per hour.

In order to verify the universality of the characteristics revealed in the previous section and the accuracy of the empirical formula, the data of the step-like deformation period in Figure 10(b) was taken as an example and the

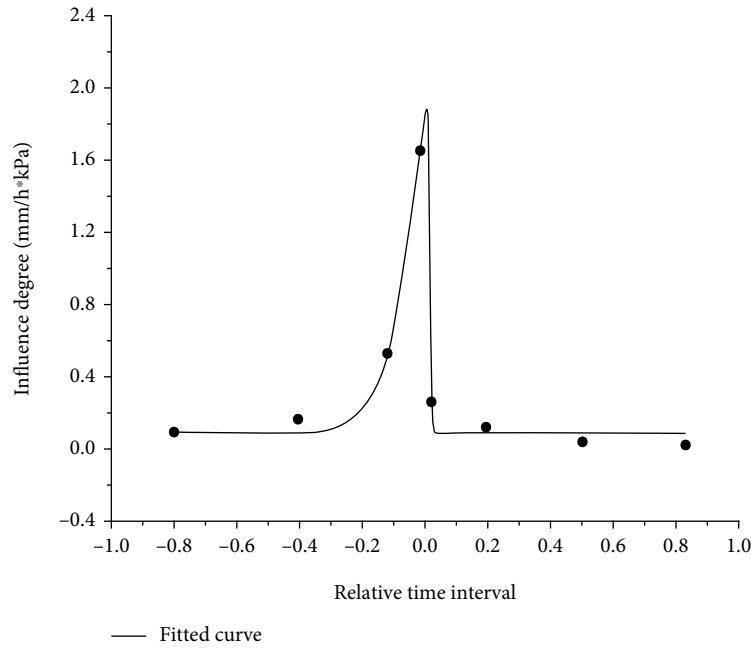


FIGURE 12: The relationship between influence degree and relative time interval.

TABLE 3: Calculated results from empirical formula of landslide displacement.

Time period	Pore-water pressure increment (kPa)	Displacement rate (mm/h)	Relative time interval	Actual influence degree (mm/h*kPa)	Calculated influence degree (mm/h*kPa)
6.84:00–6.811:00	5.5	0.299	-0.934	0.054	0.086
6.8 11:00–6.9 15:00	4.3	0.274	-0.604	0.064	0.086
6.9 15:00–6.10 9:00	1.4	0.464	-0.170	0.331	0.316
6.10 9:00–6.12 9:00	-3.2	0.218	0.098	0.068	0.086
6.12 9:00–6.14 9:00	-2.5	0.087	0.294	0.035	0.086
6.14 9:00–6.20 14:00	-5.4	0.033	0.696	0.006	0.086

following periods were selected for calculation of the influence degree. The selected periods and the calculated results are shown in Table 3. It can be seen from Table 3 that the trend revealed in the previous section also applies to this period. For example, at similar relative time intervals (-0.170 vs. 0.098), each pore-water pressure increase in the rising stage caused more landslide displacement per hour (0.331 mm) than that in the pore-water pressure dissipating stage (0.068 mm). The closer the time interval to the peak pore-water pressure (relative time intervals of -0.934, -0.604, and -0.170, respectively), the larger is the displacement caused by each pore-water pressure increment (displacement of 0.054 mm, 0.064 mm, 0.331 mm, respectively) per hour, etc. Therefore, there is a correlation between pore-water pressure change and revealed displacement. According to the data shown in Figure 12 and the actual

influence degrees shown in Table 3, it can be deduced that the formula can more accurately calculate the displacement caused by per unit of pore-water pressure increment in unit time for different time points near the peak pore-water pressure, which is consistent with the actual displacement characteristic. Because the landslides more often produce large displacements in the period close to the peak pore-water pressure, the characteristics and empirical formula revealed in this study are of theoretical and practical significance for predicting landslide displacement trends and suggesting an early warning of landslide.

Because the interaction between soil particles is mainly influenced by pore-water pressure and there are many dominant channels formed in the debris along with the decay of vegetation roots in the study area (when the dominant channels are blocked by soil particles due to seepage, the pore-

water pressure rises rapidly in a short time, having a direct impact on the landslide displacement), selecting the index of pore-water pressure instead of groundwater level to explore its relationship with displacement will be more meaningful for the analysis of a landslide mechanism and proposing an early warning for landslide in the study area, although the changes in groundwater level and pore-water pressure show a certain similarity.

6. Conclusions

The case study of the Yaoshan landslide disaster site in Anxi County, Quanzhou City, Fujian Province, was performed to reveal the infiltration pathways of rainwater, the main influencing factors (e.g. groundwater), the characteristics of pore-water pressure, and its relationship with the displacements in the step-like landslide in the study area. The data of moisture content, groundwater level, pore-water pressure, and displacement during the rainy periods were also utilized. A quantitative formula was further proposed for analyzing the effect of pore-water pressure increment on landslide displacement. The conclusions obtained from the study are as follows:

- (1) There are mainly two ways of infiltration in the landslide area under study: vertical infiltration through the slope surface and the tension cracks at the trailing edge of the landslide along with dominant channels in the soil. With the help of these infiltration pathways, rainfall quickly infiltrates into the soil, leading to a rapid rise in the groundwater level and pore-water pressure, causing adverse effects on the slopes. The pore-water pressure at a depth more than the groundwater level is mainly controlled by the influence of the groundwater level, which was mostly consistently reflected in its response time to the rainfall and amplitude change. Despite the changes in groundwater level and pore-water pressure showing some similarity, the relationship between pore-water pressure and displacement was more meaningful for analyzing the landslide in the study area
- (2) The response time of the displacement to the pore-water pressure near the slip surface and nearby location is shorter than the response time at the further distances above the slip surface. There is a correlation between the displacement and the pore-water pressure: as the pore-water pressure rises from the starting point to the peak and then dissipates to the vicinity of the starting point, the slope in the landslide zone produces a step-like displacement; in the rising stage of pore-water pressure, the displacement rate keeps increasing; in the dissipating stage of pore-water pressure, the displacement rate keeps decreasing
- (3) The correlation between the pore-water pressure change and landslide's slope displacement is revealed. An empirical formula is also proposed to

characterize the displacement produced by per unit of pore-water pressure increment in unit time. The various correlations and the formula show that the closer of the time interval to the peak pore-water pressure will generate the greater slope displacement by per unit rise in pore-water pressure in unit time. When the pore-water pressure is in the rising stage, the displacement produced by per unit increment of pore-water pressure in unit time will be larger than that in the dissipating stage of the pore-water pressure

Data Availability

The datasets used during the current study are available from the corresponding author on reasonable request.

Conflicts of Interest

The authors declare that there is no conflict of interest regarding the publication of this paper.

Acknowledgments

This work was supported by the National Natural Science Foundation of China (Nos. 41861134011 and U2005205).

References

- [1] F. Chen, H. C. Jia, E. Y. Du, L. Wang, N. Wang, and A. Q. Yang, "Spatiotemporal variations and risk analysis of Chinese typhoon disasters," *Sustainability*, vol. 13, no. 4, p. 2278, 2021.
- [2] Y. L. Cui, J. H. Hu, C. Xu, J. Zheng, and J. B. Wei, "A catastrophic natural disaster chain of typhoon-rainstorm-landslide-barrier lake-flooding in Zhejiang Province, China," *Journal of Mountain Science*, vol. 18, no. 8, pp. 2108–2119, 2021.
- [3] Y. Huang and H. L. Cheng, "The impact of climate change on coastal geological disasters in southeastern China," *Natural Hazards*, vol. 65, no. 1, pp. 377–390, 2013.
- [4] R. Andrewwinner and S. S. Chandrasekaran, "Investigation on the failure mechanism of rainfall-induced long-runout landslide at Upputhode, Kerala state of India," *Land*, vol. 10, no. 11, p. 1212, 2021.
- [5] W. Mu, X. Wu, C. Qian, and K. Wang, "Triggering mechanism and reactivation probability of loess-mudstone landslides induced by rainfall infiltration: a case study in Qinghai Province, Northwestern China," *Environment and Earth Science*, vol. 79, no. 1, pp. 1–19, 2020.
- [6] L. Hungchou, Y. Yuzhen, L. Guangxin, and P. Jianbing, "Developing processes of rainfall-induced retrogressive landslide by model experiments," *Disaster Advances*, vol. 5, no. 4, pp. 861–865, 2012.
- [7] Q. H. Ran, Y. Y. Hong, W. Li, and J. H. Gao, "A modelling study of rainfall-induced shallow landslide mechanisms under different rainfall characteristics," *Journal of Hydrology*, vol. 563, pp. 790–801, 2018.
- [8] S. W. Sun, B. Pang, J. B. Hu, Z. X. Yang, and X. Y. Zhong, "Characteristics and mechanism of a landslide at Anqian iron mine, China," *Landslides*, vol. 18, no. 7, pp. 2593–2607, 2021.

- [9] S. Q. Lu, Q. L. Yi, W. Yi, H. F. Huang, and G. D. Zhang, "Analysis of deformation and failure mechanism of Shuping landslide in Three Gorges reservoir area," *Rock and Soil Mechanics*, vol. 35, no. 4, pp. 1123–1130, 2014.
- [10] R. Ye, X. Fu, F. Guo et al., "Deformation characteristics and mechanism analysis of geological hazards during operation period of Three Gorges reservoir," vol. 29, pp. 680–692, 2021.
- [11] Z. Yiyue, Y. Kunlong, C. Lixia, L. Shuhao, L. Xin, and T. Mengjiao, "Characteristics and mechanism of spatio-temporal difference deformation of Zengjiapeng landslide," *Bulletin of Geological Science and Technology*, vol. 39, no. 2, pp. 148–157, 2020.
- [12] M. Bordoni, C. Meisina, R. Valentino, N. Lu, M. Bittelli, and S. Chersich, "Hydrological factors affecting rainfall-induced shallow landslides: from the field monitoring to a simplified slope stability analysis," *Engineering Geology*, vol. 193, pp. 19–37, 2015.
- [13] Y. Wang, T. Mao, Y. Xia, X. Li, and X. Yi, "Macro-meso fatigue failure of bimrocks with various block content subjected to multistage fatigue triaxial loads," *International Journal of Fatigue*, vol. 163, p. 107014, 2022.
- [14] N. J. Finnegan, J. P. Perkins, A. L. Nereson, and A. L. Handwerker, "Unsaturated flow processes and the onset of seasonal deformation in slow-moving landslides," *Journal of Geophysical Research - Earth Surface*, vol. 126, no. 5, pp. 1–24, 2021.
- [15] R. Vassallo, G. M. Grimaldi, and C. Di Maio, "Pore water pressures induced by historical rain series in a clayey landslide: 3D modeling," *Landslides*, vol. 12, no. 4, pp. 731–744, 2015.
- [16] K. P. Acharya, N. P. Bhandary, R. K. Dahal, and R. Yatabe, "Seepage and slope stability modelling of rainfall-induced slope failures in topographic hollows," *Geomatics, Natural Hazards and Risk*, vol. 7, no. 2, pp. 721–746, 2016.
- [17] Y. Wang, Y. Su, Y. Xia, H. Wang, and X. Yi, "On the effect of confining pressure on fatigue failure of block-in-matrix soils exposed to multistage cyclic triaxial loads," *Fatigue & Fracture of Engineering Materials & Structures*, vol. 45, no. 9, pp. 2481–2498, 2022.
- [18] V. Senthilkumar, S. S. Chandrasekaran, and V. B. Maji, "Rainfall-induced landslides: case study of the Marappalam landslide, Nilgiris District, Tamil Nadu, India05018006," *International Journal of Geomechanics*, vol. 18, no. 9, 2018.
- [19] S. R. Hencher, "Preferential flow paths through soil and rock and their association with landslides," *Hydrological Processes*, vol. 24, no. 12, pp. 1610–1630, 2010.
- [20] Y. Wang, J. Han, Y. Xia, and D. Long, "New insights into the fracture evolution and instability warning predication for fissure-contained hollow-cylinder granite with different hole diameter under multi-stage cyclic loads," *Theoretical and Applied Fracture Mechanics*, vol. 119, article 103363, 2022.
- [21] M. Zhang, L. Yang, X. Ren et al., "Field model experiments to determine mechanisms of rainstorm-induced shallow landslides in the Feiyunjiang River basin, China," *Engineering Geology*, vol. 262, article 105348, 2019.
- [22] Z. P. Zhang, X. Fu, Q. Sheng, Y. Du, Y. Zhou, and J. Huang, "Stability of cracking deposit slope considering parameter deterioration subjected to rainfall," *International Journal of Geomechanics*, vol. 21, no. 7, article 05021001, 2021.